

Supplementary Figures:

Figure 1. HFD treatment increases both hepatic and plasma triglycerides. (A) Oil-Red staining showing that HFD treatment led to increased hepatic lipid accumulation in mice. Lipid droplets in livers were labeled with arrows. (B,C) HFD treatment led to high levels of hepatic and plasma triglycerides. Lipids were extracted from the livers of mice treated with standard diet (n=6) or HFD (n=6) and triglycerides measured using a colorimetric assay. Representative histological images are shown. Data are expressed as mean \pm SD. Mann-Whitney was used for statistical analysis. (D) HFD treatment led to reduced expression of *Hbp1* in livers of dietary obese mice. Data are expressed as mean \pm SD. Mann-Whitney was used for statistical analysis.

Supplementary Figure 1

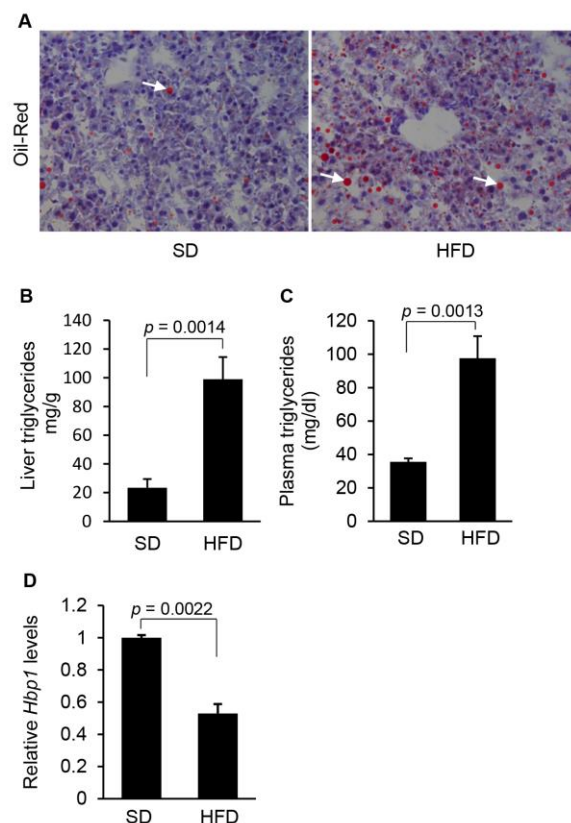


Figure 2. (A) Overexpression of *p53* caused dose-dependent inhibition of the activity of a luciferase reporter gene linked to the *Srebp1c* promoter. (B) *p53* knockdown via its siRNA released the inhibitory effect of *p53* on *Srebp1c* transcription, which was reflected by increased luciferase activity. Data are expressed as mean \pm SD. In this multiple-groups experiment, we only performed comparison between two groups and Student T test was used for statistical analysis.

Supplementary Figure 2

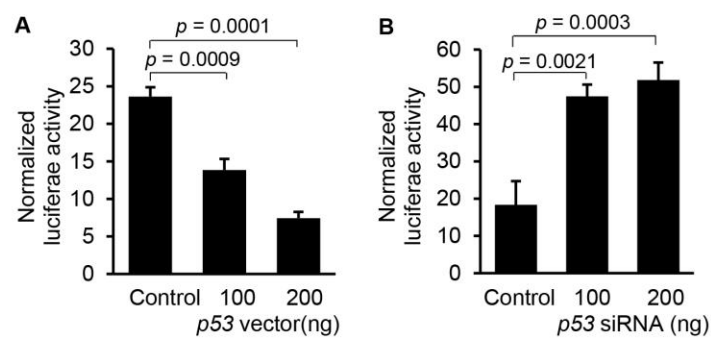


Figure 3. miR-21 modulates lipid accumulation in HepG2 cells by interacting with *p53*. (A, B) Transfection of miR-21 mimic into HepG2 cells incubated with oleate led to increased intracellular lipid content, and additional overexpression of *p53* offset the effect of miR-21. Lipid droplets in human hepatocytes were labeled with arrows. Data are expressed as mean \pm SD. Student T test was used for statistical analysis. (C,D) miR-21 inhibitor transfection into HepG2 cells cultured with the medium containing 0.5 mM oleate led to a decrease in intracellular lipid content, and additional treatment of *p53* siRNA antagonized the effect of miR-21 inhibitor on lipid accumulation. Lipid droplets in human hepatocytes were labeled with arrows. Data are expressed as mean \pm SD. Student T test was used for statistical analysis. (E) Mechanically, miR-21 inhibitor treatment induced expression of *p53* and additional transfection of *p53* siRNA into HepG2 cells knocked down induced *p53*. Briefly, HepG2 cells were cultured with DMEM containing 0.5 mM oleate. 24 hours after miR-21 inhibitor transfection, *p53* siRNA was further introduced into HepG2 cells in attempt to knock down *p53* induced by miR-21 inhibitor. Data are expressed as mean \pm SD. Student T test was used for statistical analysis.

Supplementary Figure 3

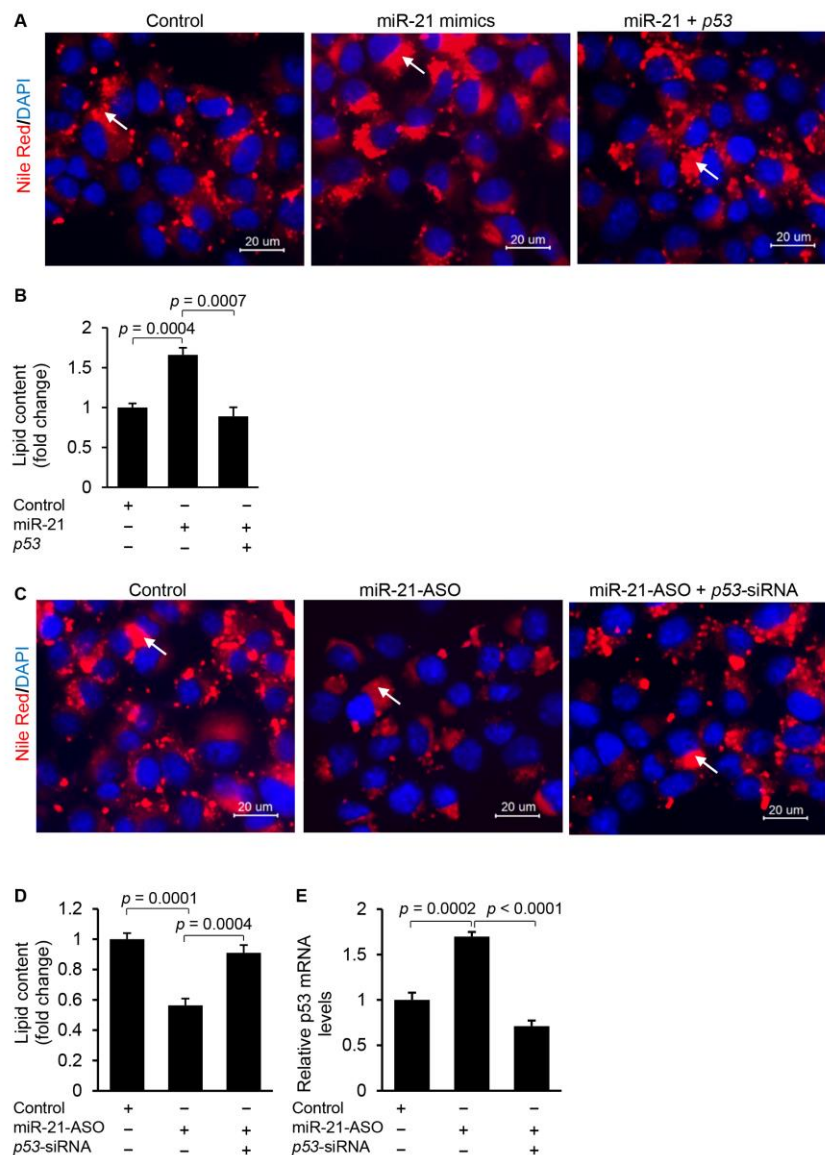


Figure 4. The inhibitory effects of miR-21-ASO on cell cycle progression and proliferation are mediated by *p53*. (A) miR-21 mimic transfection into HepG2 cells inhibited expression of *p53*, and treatment of *p53* expression vector significantly increased expression of *p53*. Data are presented as mean \pm SD. Student T test was used for statistical analysis. (B) MTT assay revealed that miR-21 overexpression induced proliferation, and overexpression of *p53* counteracted the inductive effect of miR-21 on proliferation. Data are presented as mean \pm SD. Student T test was used for statistical analysis. (C) Soft agar colony formation assay revealed that miR-21 overexpression promoted the colony formation of HepG2 cells, and further overexpression of *p53* antagonized the effect of miR-21. Data are presented as mean \pm SD. Student T test was used for statistical analysis. (D,E) miR-21 mimic treatment led to a decrease in the number of cells in the G1 phase but an increase in the number of cells in S phase, and additional overexpression of *p53* antagonized the effect of miR-21. Quantification of the cell cycle phase distribution was analyzed by flow cytometry. The proliferation index was increased in the miR-21 mimic-treated HepG2 cells and overexpression of *p53* offset the effect of miR-21. Data are presented as mean \pm SD (* p < 0.05, ** p < 0.001, Chi-Square Test). (F) miR-21 inhibitor transfection into HepG2 cells induced expression of *p53*, and additional knockdown of induced *p53* with its siRNA inhibited expression of *p53*. Specifically, HepG2 cells were treated with oleate (0.5 mM) to induce miR-21, and then miR-21-ASO was transfected into HepG2 cells to knock down upregulated miR-21. Levels of *p53* were determined by qRT-PCR. Data are presented as mean \pm SD. Student T test was used for statistical analysis. (G) MTT assay revealed that antagonizing miR-21 via miR-21 inhibitor led to reduced cellular proliferation in HepG2 cells, and additional knockdown of *p53* by its siRNA rescued the effect of miR-21 inhibitor. Data are presented as mean \pm SD. Student T test was used for statistical analysis. (H) Soft agar colony formation assay revealed that miR-21 knockdown inhibited the growth of HepG2 cells, and the additional treatment of *p53*-siRNA antagonized the effect of miR-21 inhibitor. Data are presented as mean \pm SD. Student T test was used for statistical analysis. (I,J) miR-21 inhibitor treatment prevented cell cycle progression, and additional knockdown of *p53* rescued the effect of miR-21 inhibitor. miR-21 knockdown increased the number of cells in the G1 phase but decreased the number of cells in S phase, and additional knockdown of up-regulated *p53* by its siRNA antagonized the effect of miR-21 inhibitor. Quantification of the cell cycle phase distribution was analyzed by flow cytometry. The proliferation index was reduced in the miR-21 inhibitor treated HepG2 cells and the additional treatment of *p53*-siRNA offset the effect of miR-21 inhibitor. Data are presented as mean \pm SD (** p < 0.001, Chi-Square Test). (K) miR-21-ASO inhibited growth of subcutaneous tumors from HepG2 cells in nude mice, and additional treatment of *p53*-siRNA counteracted the effect of miR-21-ASO. HepG2 cells treated with scramble control, miR-21-ASO or a combination of miR-21-ASO and *p53*-siRNA were injected subcutaneously into nude mice. Data represent mean \pm SD. Mann-Whitney was used for statistical analysis of tumor weight.

Supplementary Figure 4

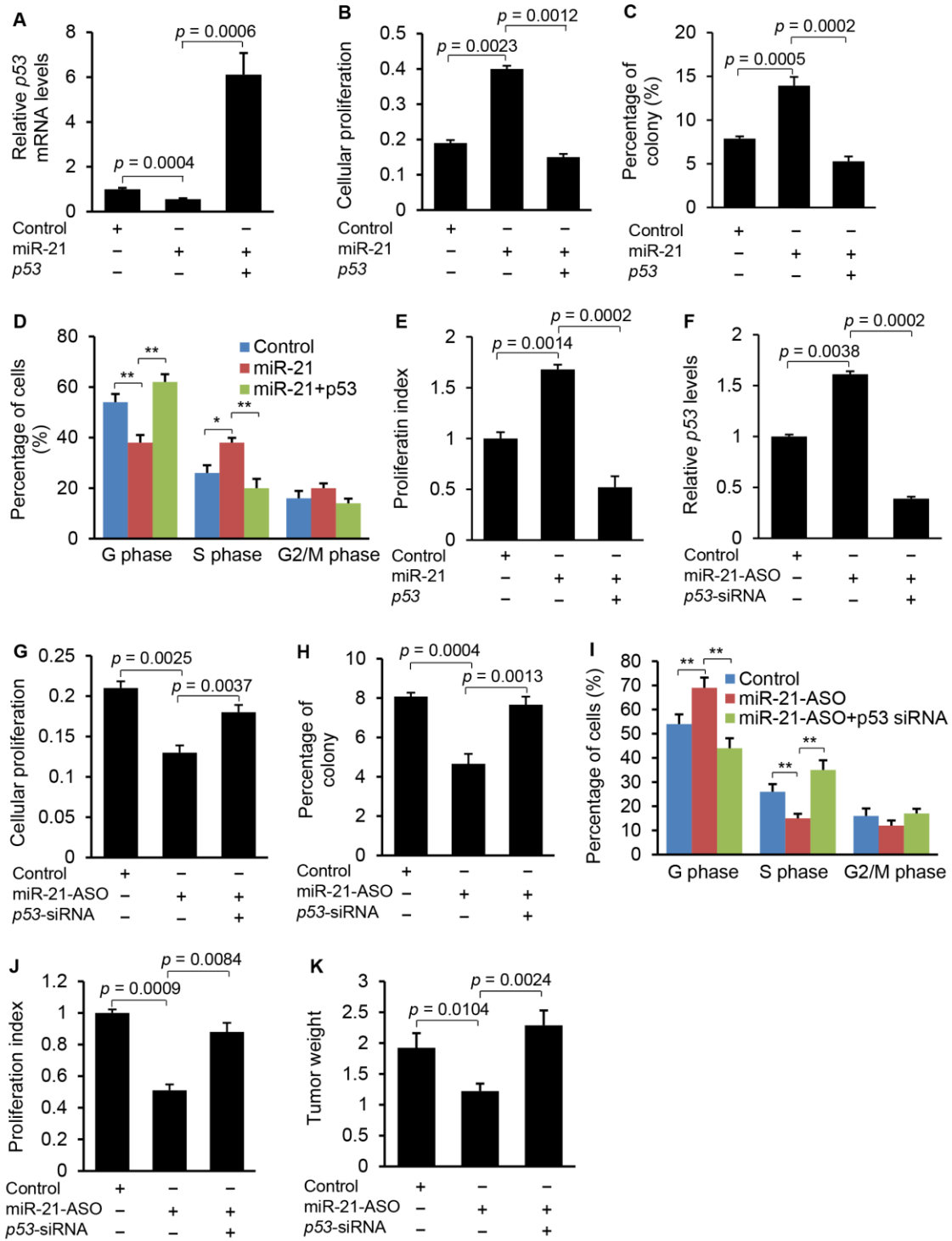


Figure 5. Knocking down miR-21 prevented hepatic lipid accumulation in HFD-treated mice. (A,B) miR-21 knockdown inhibited lipid accumulation in livers of HFD-fed mice injected with miR-21-ASO. Representative images (Oil-Red) are shown. Lipid droplets in livers were labeled with arrows. Cellular triglyceride content was measured by Oil Red staining and triglyceride (TG) content (per mg protein) was measured with a triglyceride estimation kit. Briefly, 8-week old mice were kept on HFD until 20 weeks of age. At 12 weeks of age, mice were divided into two groups: one group (n=8) received miR-21-MM-ASO and the other group received miR-21-ASO for another eight weeks. (C) miR-21-ASO injection into dietary obese mice resulted in down-regulated miR-21 and increased *Hbp1* and *p53* expression. Data represent mean \pm SD. Mann-Whitney was used for statistical analysis. * $p < 0.05$.

Supplementary Figure 5

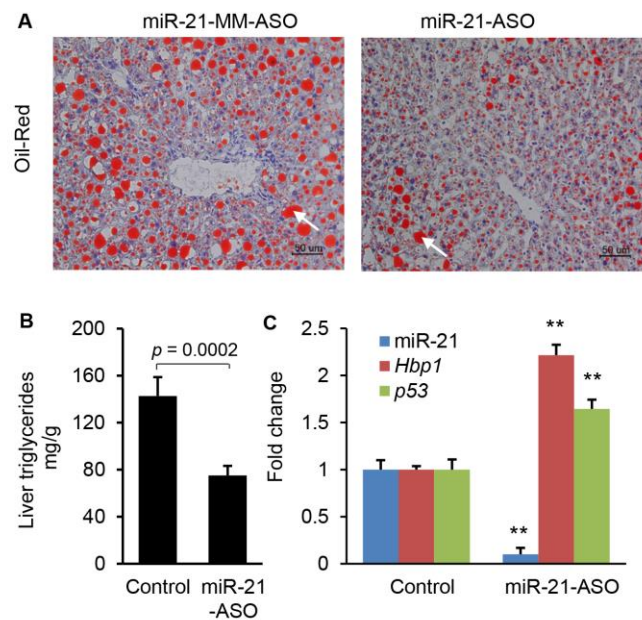


Figure 6. miR-21 knockdown had no effect on serum free fatty acid and glycerol as well as the expression of the genes encoding enzymes for fatty acid oxidation. (A,B) miR-21-ASO treatment had no effect on levels of serum free fatty acid and glycerol in dietary obese mice. (C) qRT-PCR revealed that miR-21 knockdown did not change the expression of β -oxidation-related genes including *Cpt1 α* , *Acc2* and *PGC1 α* .

Supplementary Figure 6

